Journal of Solid Mechanics Vol. 12, No. 2 (2020) pp. 455-475
DOI: 10.22034/jsm.2019.1873720.1466

Effect of Winkler Foundation on Radially Symmetric Vibrations of Bi-Directional FGM Non-Uniform Mindlin's Circular Plate Subjected to In-Plane Peripheral Loading

N. Ahlawat [1, *], R. Lal [2]

[1]*Department of Mathematics, Jaypee Institute of Information Technology, Noida, India*
[2]*Department of Mathematics, Indian Institute of Technology Roorkee, Roorkee, India*

Received 21 March 2020; accepted 18 May 2020

ABSTRACT

An analysis has been presented of the effect of elastic foundation and uniform in-plane peripheral loading on the natural frequencies and mode shapes of circular plates of varying thickness exhibiting bi-directional functionally graded characteristics, on the basis of first order shear deformation theory. The material properties of the plate are varying following a power-law in both the radial and transverse directions. The numerical solutions of the coupled differential equations leading the motion of simply supported and clamped plates acquired by using Hamilton's principle, is attained by harmonic differential quadrature method. The effect of different plate parameters namely gradient index, heterogeneity parameter, density parameter, taper parameter and thickness parameter is illustrated on the vibration characteristics for the first three modes of vibration for various values of in-plane peripheral loading parameter together with foundation parameter. Critical buckling loads in compression are calculated for both the boundary conditions by putting the frequencies to zero. The reliability of the present technique is confirmed by comparing the results with exact values and results of published work.

Keywords: First order shear deformation theory; Buckling; Functionally graded circular plates; Harmonic differential quadrature; Axisymmetric vibrations.

1 INTRODUCTION

FUNCTIONALLY graded materials (FGMs) previously used as thermal barrier materials and now, they are used in general as a structural component in high temperature environments such as nuclear reactor technology, spacecraft heat shields, gas turbines, high speed aerospace vehicles, biomaterial electronics, armor protection for

*Corresponding author.
E-mail address: ahlawatneha@gmail.com (N. Ahlawat).

military applications etc. (Miyamoto et al., [31]). FGMs are a class of composites that have gradual but continuous variation of material properties from one surface to the other. Typical FGMs are made from a combination of ceramic and metal. The metal prevents fracture because of its higher toughness while ceramic high-temperature resistance because of its low thermal conductivity. Motivated by enormous engineering applications, FGMs have attracted a number of researchers to analyze the static and dynamic behaviour of plates made of these materials. Vibrational characteristics of FGM/non-FGM plate-type structural components have been studied by many workers using different plate theories: classical plate theory (CPT) (Efraim, [10]; Baferani et al., [3]), first order shear deformation theory (FSDT) (Irie et al., [24]; Su et al., [39]), higher order shear deformation theory (HSDT) (Batra and Aimmanee, [4]; Bisadi et al., [5]) etc. Among these, the FSDT proposed by Mindlin (Mindlin, [30]), gives sufficiently accurate results for moderately thick plates by including the effects of rotatory inertia and transverse shear. In this regard, a number of studies are existing in the literature and significant ones are given in (Liew et al.,[29]; Han and Liew, [19]; Ferreira et al., [14]; Civalek, [8]; Hosseini-Hashemi et al., [22]; Saidi et al., [36]; Zamani et al., [48]; Eftekhari and Jafari, [12]; Xue et al., [47]; Chen et al., [7], Wang et al., [44]). Out of these, Liew et al. [29]) have predicted the frequency parameters for thick isotropic rectangular plates using Ritz energy method with orthogonal polynomials. Han and Liew [19] have analysed the axisymmetric free vibrations of moderately thick annular plates using differential quadrature method. Ferreira et al. [14] have used multiquadric radial basis function procedure to study the free vibration performance of moderately thick symmetrically laminated composite square and skew plates. The discrete singular convolution method has been developed by Civalek [8] for free vibration analysis of moderately thick symmetrically laminated composite rectangular plates. Hosseini-Hashemi et al. [22] have obtained closed-form solutions for analyzing free vibration of annular and circular FGM plates using Bessel functions. Benchmark solutions for free vibration analysis of moderately thick annular sector plates have been presented by Saidi et al. [36] using Bessel functions. Zamani et al. [48] have investigated free vibration of moderately thick symmetrically laminated trapezoidal plates with different combinations of boundary conditions employing generalized differential quadrature method. Eftekhari and Jafari [12] have projected a modified mixed Ritz-differential quadrature formulation to study the vibration of thick skew and rectangular plates. An improved Fourier series method has been used to study the free vibration of Mindlin rectangular plates with elastic boundary supports by Xue et al. [47]. A meshless local natural neighbour interpolation method has been used by Chen et al.[7] to obtain the natural frequencies of moderately thick FGM rectangular, triangular and skew plates. Very recently, a comprehensive review on various plate theories for FGM plates and shells has been presented by Thai and Kim[42].

Plates resting on an elastic foundation find their wide applications in modern engineering structures and their use in building footings, reinforced concrete pavements of high runways, storage tanks, indoor games, base of machines, airport runways, buried pipelines, bridge decks and submerged floating tunnels etc. are very common. Keeping this in view, various foundation models have been proposed in the literature (Bowles, [6]). Out of these, the most commonly used model is Winkler's model which gives acceptable results in a variety of physical problems (Xiang,[45]; Gupta et al., [17]; Amini et al., [1]; Li and Yuan, [28]; Fallah et al., [13]; Rao and Rao, [35]; Zhang et al., [50]), to mention a few. Of these, first-known exact solutions for the vibration of rectangular Mindlin plates resting on non-homogenous Winkler foundation have been presented by Xiang et al. [45]). Three-dimensional free vibration analyses of rectangular FGM plates resting on Winkler foundation have been done by Amini et al. [1] using Chebyshev polynomials and Ritz method. Fallah et al. [13] have studied the free vibration analysis of moderately thick rectangular FGM plates resting on Winkler foundation employing extended Kantorovich method together with infinite power series solution. Very recently, Zhang et al. [50] have explored the element-free improved moving least-squares Ritz method in computing the vibration solution of thick FG carbon-nanotube-reinforced composite plates resting on Winkler foundation. In normal situations, these plates can be subjected to in-plane stressing which arises due to variety of stresses: centrifugal, hydrostatic and thermal etc. (Gupta and Lal,[16]; Leissa,[27]; Gorman, [15]), which may provoke a highly undesirable phenomenon of buckling. This necessitates studying the buckling behaviour of plates of different geometries with a fair amount of accuracy. The exact solutions for the vibration and buckling of stepped rectangular Mindlin plates have been obtained by Xiang and Wei [46] using combination of domain decomposition and Levy-type method. The sinusoidal shear deformation plate theory is used by Zenkour [49] to analyze the buckling and free vibration behaviour of simply supported FG sandwich plate. Closed form solution for the buckling of circular FGM plates under uniform compression on the basis of higher order shear deformation theory (HSDT) has been obtained by Najafizadeh and Heydari [33]. Element-free *kp*-Ritz method has been used by Zhao et al. [52] in analyzing two types of buckling of FGM plates having arbitrary geometry, together with the plates having square and circular holes at the centre. Bessel functions have been used in obtaining an analytical solution for buckling of moderately thick functionally graded sectorial plates by Naderi and Saidi [32]. Generalized differential quadrature method has been employed by Ansari et al. [2] for thermal buckling analysis of a Mindlin rectangular FG microplate based on strain gradient theory. Very recently, the buckling

behaviour of functionally graded carbon nanotube reinforced composite thick skew plates has been studied by Zhang et al. [51] employing element-free interpolating moving least-squares-Ritz method. Further, with suitable variation of thickness, these plates in the existence of the elastic foundation and axial forces are of great use in many engineering applications: mainly in ship buildings, automotive industry, telephone industry, aerospace industry etc., due to the potential savings on material usage, reduction in weight and increase in the stiffness. Regarding this, an exact element technique has been developed by Efraim and Eisenberger [11] to study the vibration behaviour of thick annular FGM and isotropic plates having different types of thickness variation on the basis of first order shear deformation theory (FSDT). The effect of elastic foundation has been presented on free vibration analysis of thin radially FGM annular and circular sector plates of non-linear thickness by Hosseini-Hashemi et al. [23] employing differential quadrature method. A study of 3-D free vibration analysis of annular and circular thick FGM plates with parabolic and linear thickness along radial direction and resting on foundation have been done by Tajeddini et al.[40] using polynomial-Ritz method. An exact closed form solution to analyze free vibration of moderately thick annular and circular FG plates of stepped thickness variation has been presented by Hosseini-Hashemi et al. [21]. Recently, free vibration of two-dimensional FGM sectorial plate with linear and non-linear thickness resting on Winkler–Pasternak elastic foundation has been studied by Satouri et al. [37] using 2-D differential quadrature method based on FSDT.

In this article, the consequence of Winkler foundation has been studied on the vibration and buckling of bi-directional moderately thick FGM circular plates subjected to uniform tensile in-plane force. The thickness of the plate vary linearly along the radial direction on the basis of FSDT and mechanical properties of the material i.e. Young's moduli and density are supposed to vary in radial (R) as well as transverse (z) directions following a power-law of the component materials. The coupled differential equations of motion for this kind of a plate model have been obtained using Hamilton's principle. Harmonic differential quadrature method has been used to get the frequency equations for simply supported (SS) and clamped (C) boundary conditions. These resultant equations are then solved using software MATLAB to get the frequency parameter. The effect of different parameters like gradient index g, in-plane peripheral loading parameter N, density parameter β, heterogeneity parameter α, taper parameter γ, thickness parameter h_0 and foundation parameter K_f has been analysed on the frequency parameter. For the two boundary conditions, critical buckling loads are obtained by putting the frequency to zero. 3D mode shapes for the initial three frequency parameters for a specific data have been drawn. For the justification of the obtained results, a comparison has been presented with the available data obtained by exact and numerical techniques.

2 MATHEMATICAL MODELLING

Assume a bi-directional circular FGM plate of mass density ρ, thickness h, radius a and subjected to a tensile uniform in-plane peripheral loading N_0. Referring to a cylindrical polar coordinate system (R, θ, z), let the upper and lower surfaces of the plate are $z = +h/2$ and $z = -h/2$, respectively. $z = 0$ and line $R = 0$ are the middle plane and axis of the plate, respectively. Following the first order shear deformation theory (Mindlin, [30]; Irie et al., [25]), the differential equations leading the free transverse axisymmetric vibration for the present problem (Fig. 1) have been derived using Hamilton's principle and are specified as under:

$$\frac{\partial M_R}{\partial R}+\frac{M_R-M_\theta}{R}-Q_R-k_1\frac{\rho h^3}{12}\frac{\partial^2\psi}{\partial t^2}=0 \tag{1a}$$

$$\frac{\partial Q_R}{\partial R}+\frac{1}{R}Q_R-N_0\frac{\partial^2 w}{\partial R^2}-\frac{N_0}{R}\frac{\partial w}{\partial R}-k_f w-\rho h\frac{\partial^2 w}{\partial t^2}=0 \tag{1b}$$

where w is the transverse deflection, t the time, k_f the Winkler foundation modulus, ψ the angle of rotation of the plate element in the R-z plane, k_1 the tracer identifying the rotatory inertia term and M_R, M_θ and Q_R are the moments and shear resultants per unit length given by

$$M_R=\int_{-h/2}^{h/2}\frac{E(R,z)}{1-\nu^2}\left[z\frac{\partial\psi}{\partial R}+\nu\frac{z}{R}\psi\right]z\,dz\quad,\quad M_\theta=\int_{-h/2}^{h/2}\frac{E(R,z)}{1-\nu^2}\left[\frac{z}{R}\psi+\nu z\frac{\partial\psi}{\partial R}\right]z\,dz$$

and

$$Q_R = \int_{-h/2}^{h/2} \kappa G \left[\psi + \frac{\partial w}{\partial R} \right] dz$$

where κ is the shear correction factor and G is the shear modulus.

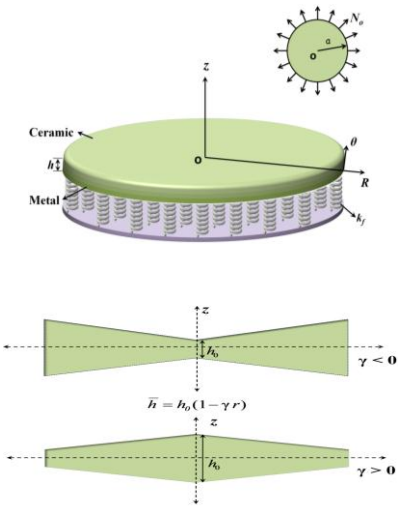

Fig.1
FGM circular plate under uniform in-plane peripheral loading N_0 and resting on Winkler foundation of moduli k_f.

Let us assume that the lower and upeer surfaces of the plate are metal and ceramic-rich, respectively. The material properties i.e. Young's moduli $E(R,z)$ and density $\rho(R,z)$ are followed by

$$E(R,z) = \left[(E_c - E_m)\left(\frac{z}{h} + \frac{1}{2} \right)^g + E_m \right] e^{\alpha \frac{R}{a}} \tag{2}$$

$$\rho(R,z) = \left[(\rho_c - \rho_m)\left(\frac{z}{h} + \frac{1}{2} \right)^g + \rho_m \right] e^{\beta \frac{R}{a}} \tag{3}$$

where E_m, ρ_m and E_c, ρ_c denote Young's moduli and density of metal and ceramic layers, respectively, g the gradient index of the material, β the density parameter and α the heterogeneity parameter.

Thus, the stress resultants becomes

$$M_R = D^* B_1 e^{\alpha \frac{R}{a}} \left[\frac{\partial \psi}{\partial R} + \nu \frac{\psi}{R} \right],\ M_\theta = D^* B_1 e^{\alpha \frac{R}{a}} \left[\frac{\psi}{R} + \nu \frac{\partial \psi}{\partial R} \right] \text{ and}$$

$$Q_R = G^* h e^{\alpha \frac{R}{a}} \left[\psi + \frac{\partial w}{\partial R} \right] B_2$$

where

$$D^* = \frac{E_c h^3}{12(1-\nu^2)},\ B_1 = \left[3\left(1 - \frac{E_m}{E_c} \right) \left\{ \frac{g^2 + g + 2}{(g+1)(g+2)(g+3)} + \frac{E_m}{E_c} \right\} \right],\ G^* = \frac{E_c}{2(1+\nu)},$$

$$B_2 = \frac{\kappa\left(1 + \left(E_m / E_c\right) g\right)}{(g+1)}$$

Substitution of these values for stress resultants in Eq. (1a) and Eq. (1b) leads to

$$D^* B_1 e^{\alpha\frac{R}{a}}\left[\frac{\alpha}{a}\left(\frac{\partial\psi}{\partial R}+\nu\frac{\psi}{R}\right)+\frac{\partial^2\psi}{\partial R^2}+\frac{1}{R}\frac{\partial\psi}{\partial R}-\frac{\psi}{R^2}\right]-G^* h e^{\alpha\frac{R}{a}} B_2\left(\psi+\frac{\partial w}{\partial R}\right)-k_1 B_3\,\rho_c\, e^{\beta\frac{R}{a}}\frac{h^3}{12}\frac{\partial^2\psi}{\partial t^2}=0 \tag{4a}$$

$$\begin{aligned}&G^* h\,\frac{\alpha}{a}\,e^{\alpha\frac{R}{a}} B_2\left(\psi+\frac{\partial w}{\partial R}\right)+G^* h\, e^{\alpha\frac{R}{a}} B_2\left(\frac{\partial\psi}{\partial R}+\frac{\partial^2 w}{\partial R^2}\right)+\frac{G^* h e^{\alpha\frac{R}{a}}}{R} B_2\left(\psi+\frac{\partial w}{\partial R}\right)-\\ &N_0\left(\frac{\partial^2 w}{\partial R^2}+\frac{1}{R}\frac{\partial w}{\partial R}\right)-k_f w-B_3\,\rho_c\, e^{\beta\frac{R}{a}} h\,\frac{\partial^2 w}{\partial t^2}=0\end{aligned} \tag{4b}$$

where $B_3=\dfrac{(\rho_c+\rho_m g)}{\rho_c(g+1)}$.

We introduce the non-dimensional variables, $H = h/a$, $r = R/a$, $\bar{w} = w/a$, $\bar{t}=t\sqrt{\dfrac{E_c}{\rho_c a^2(1-\nu^2)}}$ together with linear thickness variation i.e. $\bar{h}=h_0(1-\gamma r)$, γ denotes the taper parameter and h_0 is the non-dimensional thickness of the plate at the centre in Eq. (4a) and (4b), one gets

$$\begin{aligned}&B_1(1-\gamma r)\left[\left\{-3\gamma+\alpha(1-\gamma r)\right\}\left(\frac{\partial\psi}{\partial r}+\nu\frac{\psi}{r}\right)+(1-\gamma r)\left(\frac{\partial^2\psi}{\partial r^2}+\frac{\nu}{r}\frac{\partial\psi}{\partial r}-\nu\frac{\psi}{r^2}\right)\right]\\ &+\frac{B_1}{r}(1-\nu)(1-\gamma r)^2\left(\frac{\partial\psi}{\partial r}-\frac{\psi}{r}\right)-\frac{6(1-\nu)}{h_0^2} B_2\left(\psi+\frac{\partial\bar{w}}{\partial r}\right)-k_1 B_3(1-\gamma r)^3 e^{(\beta-\alpha)r}\frac{\partial^2\psi}{\partial\bar{t}^2}=0\end{aligned} \tag{5a}$$

$$\begin{aligned}&G^* h_0 B_2 e^{\alpha r}\left[\left\{-2\gamma+\alpha(1-\gamma r)+\frac{1}{r}\right\}\left(\psi+\frac{\partial\bar{w}}{\partial r}\right)+(1-\gamma r)\left(\frac{\partial\psi}{\partial r}+\frac{\partial^2\bar{w}}{\partial r^2}\right)\right]\\ &-\frac{N_0}{a}\left(\frac{\partial^2\bar{w}}{\partial r^2}+\frac{1}{r}\frac{\partial\bar{w}}{\partial r}\right)-k_f\bar{w}\,a-\frac{B_3 h_0(1-\gamma r)e^{\beta r}E_c}{(1-\nu^2)}\frac{\partial^2\bar{w}}{\partial\bar{t}^2}=0\end{aligned} \tag{5b}$$

For harmonic vibrations, the solutions can be considered as:

$$\bar{w}(r,\bar{t})=W(r)e^{i\lambda\bar{t}} \quad \text{and} \quad \psi(r,\bar{t})=\Psi(r)e^{i\lambda\bar{t}} \tag{6}$$

The Eq. (5a) and (5b) reduces to

$$U_1\frac{d^2\Psi}{dr^2}+U_2\frac{d\Psi}{dr}+\left[U_3+k_1U_4\lambda^2\right]\Psi+U_5\frac{dW}{dr}=0 \tag{7a}$$

$$V_1\frac{d^2W}{dr^2}+V_2\frac{dW}{dr}+\left[V_3\lambda^2+V_4\right]W+V_5\frac{d\Psi}{dr}+V_6\Psi=0 \tag{7b}$$

where

$$U_1=B_1(1-\gamma r)^2,\quad U_2=B_1(1-\gamma r)\left[-3\gamma+(1-\gamma r)\left(\alpha+\frac{1}{r}\right)\right],$$

$$U_3 = B_1(1-\gamma r)\left[\frac{-3\nu\gamma}{r}+\frac{(1-\gamma r)}{r}\left(\alpha\nu-\frac{1}{r}\right)\right]-\frac{6(1-\nu)B_2}{{h_0}^2},\ U_4 = B_3(1-\gamma r)^2 e^{(\beta-\alpha)r},$$

$$U_5 = -\frac{6(1-\nu)B_2}{{h_0}^2},\ V_1 = (1-\gamma r)-\frac{N}{B_2}e^{-\alpha r},\ V_2 = -\gamma+\left(\alpha+\frac{1}{r}\right)(1-\gamma r)-\frac{N}{r\,B_2}e^{-\alpha r},$$

$$V_3 = \frac{2B_3(1-\gamma r)e^{(\beta-\alpha)r}}{B_2(1-\nu)},\ V_4 = -\frac{K_f}{B_2}e^{-\alpha r},\ V_5 = (1-\gamma r),\ V_6 = -\gamma+(1-\gamma r)\left(\alpha+\frac{1}{r}\right),$$

$$N = \frac{N_0}{G^* a\, h_0},\ K_f = \frac{k_f a}{G^* h_0}$$

The non-dimensional frequency parameter Ω has been taken for the presentation of the results and defined as:

$$\Omega = \omega a^2\sqrt{\frac{\rho_c\, h}{D^*}} \quad \text{where} \quad \omega = \lambda\sqrt{\frac{E_c}{\rho_c\, a^2(1-\nu^2)}}$$

Eq. (7a) and (7b) are coupled linear equations with variable coefficients. The numerical solution with suitable regularity and boundary conditions at the centre has been obtained using harmonic differential quadrature method (HDQM).

2.1 Boundary conditions

(i) SS-edge

$$W = 0,\ \left(\frac{d\,\Psi}{d\,r}+\nu\frac{\Psi}{r}\right)=0 \tag{8}$$

(ii) C-edge

$$\Psi = 0,\quad W = 0 \tag{9}$$

2.2 *Regularity condition*

The regularity condition of the plate at the centre ($r = 0$) for axisymmetric boundary conditions can be written as:

$$\Psi = 0,\quad Q_r = 0 \tag{10}$$

3 METHOD OF SOLUTION

Let $r_1, r_2, ..., r_m$ be the *m* grid points in the suitable interval [0, 1] of the plate and according to HDQM (Striz et al.,[38]), the n^{th} order derivatives of $W(r)$ and $\Psi(r)$ with respect to *r* at the i^{th} point r_i are given by

$$\left(W_r^{(n)}(r_i), \Psi_r^{(n)}(r_i)\right) = \sum_{j=1}^{m} C_{ij}^{(n)}\left(W(r_j), \Psi(r_j)\right), \quad \text{for } i = 1,2,\ldots m \tag{11}$$

where $C_{ij}^{(n)}$ are the weighting coefficients.

The weighting coefficients of first order i.e. $C_{ij}^{(1)}$ are given as:

$$C_{ij}^{(1)} = \frac{(\pi/2)L^1(r_i)}{L^1(r_j)\sin\{(r_i - r_j)\pi/2\}}$$

where

$$L^1(r_i) = \prod_{j=1, j\neq i}^{m} \sin\left\{\frac{(r_i - r_j)\pi}{2}\right\}, \qquad \text{for} \quad i, j = 1,2,...,m \text{ . but } j \neq i$$

The second order weighting coefficients are obtained from the following recurrence relations

$$C_{ij}^{(2)} = C_{ij}^{(1)}\left(2C_{i1}^{(1)} - \pi\cot\left\{\frac{(r_i - r_j)\pi}{2}\right\}\right), \quad \text{for } i, j = 1(1)m, \quad \text{but } i \neq j \quad \text{and} \quad n = 2,3,...$$

with $C_{ii}^{(n)} = -\sum_{j=1, j\neq i} C_{ij}^{(n)}$, for $i = 1(1)m$, $n \geq 1$.

The third and fourth order weighting coefficients have been computed from $C_{ij}^{(1)}$ and $C_{ij}^{(2)}$ by using the following relations:

$$C_{ij}^{(3)} = \sum_{k=1}^{m} C_{ik}^{(1)} C_{kj}^{(2)} \quad \text{and} \quad C_{ij}^{(4)} = \sum_{k=1}^{m} C_{ik}^{(2)} C_{kj}^{(2)}$$

The weighting coefficients have been obtained after selecting a particular grid point distribution which is Chebyshev–Gauss–Lobatto grid points distribution for the current problem. Hence, the coordinates of the grid points r_i are:

$$r_i = \frac{1}{2}\left[1 - \cos\left(\frac{i-1}{m-1}\pi\right)\right], \text{ for } i = 1(1)m$$

Discretizing Eq. (7a) and (7b) at the grid points $r = r_i$, $i = 2(1)(m\text{-}1)$ and putting the values of first two derivatives of $W(r)$ and $\Psi(r)$ from Eq. (11), we get

$$\sum_{j=1}^{m}\left(U_{1,i} C_{ij}^{(2)} + U_{2,i} C_{ij}^{(1)}\right)\Psi(r_j) + \left[U_{3,i} + k_1 U_{4,i}\lambda^2\right]\Psi(r_i) + \sum_{j=1}^{m} U_{5,i} C_{ij}^{(1)} W(r_j) = 0 \tag{12a}$$

$$\sum_{j=1}^{m}\left(V_{1,i} C_{ij}^{(2)} + V_{2,i} C_{ij}^{(1)}\right)W(r_j) + \left[V_{3,i}\lambda^2 + V_{4,i}\right]W(r_i) + \sum_{j=1}^{m} V_{5,i} C_{ij}^{(1)}\Psi(r_j) + V_{6,i}\Psi(r_i) = 0 \tag{12b}$$

The boundary and regularity conditions (8-10) in their discretized forms are:
SS-edge condition

$$W(r_m) = 0, \quad \sum_{j=1}^{m} C_{ij}^{(1)}\Psi(r_j) + \nu\,\Psi(r_m) = 0 \tag{13}$$

C-edge condition

$$\Psi(r_m) = 0, \quad W(r_m) = 0 \tag{14}$$

Regularity condition

$$\Psi(r_1)=0, \quad \Psi(r_1)+\sum_{j=1}^{m} C_{i\,j}^{(1)} W(r_1)=0 \tag{15}$$

The satisfaction of Eq. (12a) and (12b) at $(m-2)$ interior grid points $r=r_i, i=2(1)(m-1)$ simultaneously with Eq. (15) gives a set of $(2m-2)$ equations in m unknowns $f_j = f(r_j),\ j=1(1)m$. The matrix form of the resultant system of equations is

$$\left[F\right]_{(2m-2)\times 2m}\left[C\right]_{2m\times 1}=\left[0\right] \tag{16}$$

In case of SS-plate, a set of 2 homogeneous equations is obtained from Eqs. (13) and (16) which provides an entire set of 2m equations in 2m unknowns for which the matrix form is:

$$\begin{bmatrix} F \\ F^S \end{bmatrix}\left[C\right]=\left[0\right] \tag{17}$$

where F^S is a $2\times 2m$ order matrix. For a non-zero solution of Eq. (17), the frequency determinant must be zero and thus:

$$\begin{vmatrix} F \\ F^S \end{vmatrix}=0 \tag{18}$$

In the same way, the frequency determinant for C-plate has been written as:

$$\begin{vmatrix} F \\ F^C \end{vmatrix}=0 \tag{19}$$

4 NUMERICAL RESULTS AND DISCUSSIONS

The values of frequency parameter Ω have been provided by the frequency Eqs. (18) and (19). The smallest three roots of these equations has been attained by using software MATLAB and noted as the frequencies for the first three modes. The effect of the rotatory inertia and transverse shear on these frequencies for different values of various parameters i.e. in-plane peripheral loading parameter N, gradient index g, thickness parameter h_0 , taper parameter γ, foundation parameter K_f, density parameter β and heterogeneity parameter α have been analysed for both the boundary conditions. To obtain the results on the basis of classical plate theory, the differential equation governing the motion is obtained by putting the tracer $k_1 = 0$ in Eq. (1a) and $\psi=-\dfrac{\partial w}{\partial R}$ in the relations for moments and shear resultants. The aluminium and alumina are chosen as an example of ceramic and metal, respectively and the numerical values of Young's moduli and density for these materials are taken (Fallah et al., [13]) as follows:

$$E_m=70\ GPa,\quad \rho_m=2,702\ kg/m^3,\ E_c=380\ GPa,\quad \rho_c=3,800\ kg/m^3$$

From the literature, the values of other parameters are:
Gradient index g = 0, 1, 3, 5;
In-plane peripheral loading parameter N = - 10, - 5, 0, 5, 10, 20;
Thickness parameter h_0 = 0.05, 0.15, 0.25;

Foundation parameter K_f = 0, 0.01, 0.02, 0.03, 0.04;
Heterogeneity parameter α = - 0.5, 0, 1;
Density parameter β = - 0.5, 0, 1;
Taper parameter γ = -0.5, 0, 0.5 and Poisson's ratio ν = 0.3.
The value of the shear correction factor κ has been taken from (Thai and Choi, [41]) as 5/6.

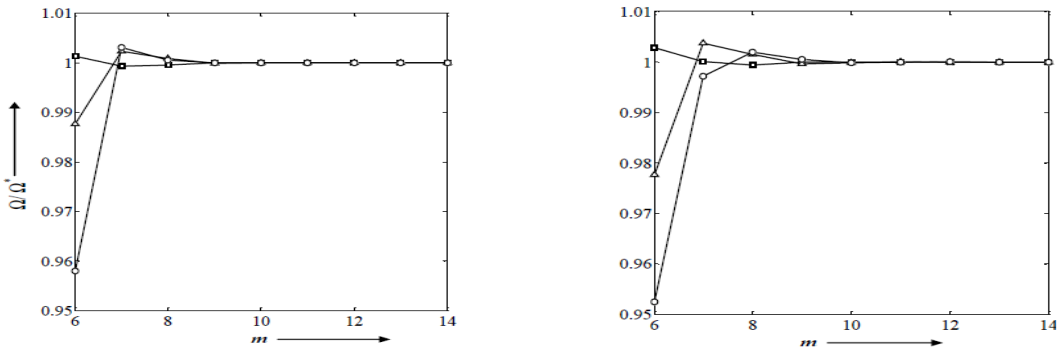

Fig.2
Convergence study of Ω/Ω^* for: (a) SS-plate (b) C-plate for K_f = 0.04, N = 20, g =5, h_0 = 0.25, α = - 0.5, β = - 0.5, γ = 0.5 ; □ , I mode; Δ , II mode; ○ , III mode.

A specific computer code was developed to calculate the frequency parameter Ω in order to select a suitable value of m and then it was executed for various sets of the values of parameters for both the plates taking m = 6, 7,…,14. After that, the following convergence criterion has been taken:

$$\left|\Omega_{m+1}^{(i)}-\Omega_{m}^{(i)}\right| \le \frac{1}{2}\times 10^{-4} \quad \text{for all the three modes } i = 1, 2, 3$$

In current problem, m has been selected as 14 for both the plates, because further increase in values of m does not advance the results. Thereafter, the normalized frequency parameter Ω/Ω^* for a specific plate N = 20, g = 5, h_0 = 0.25, K_f = 0.04, α = - 0.5, β = - 0.5, γ = 0.5 has been shown in Fig. 2, as maximum variations were observed for this data where Ω^* is the value of Ω for m = 14.

Table 1
Comparison of frequency parameter Ω for homogeneous (α = 0, β = 0) isotropic (g = 0) Mindlin circular plates for N = 0, K_f = 0, γ = 0.

Refs.	SS			C		
	I	II	III	I	II	III
			h_0 = 0.25			
Present	4.6963	23.2541	46.7745	8.8068	27.2529	49.4204
Irie et al. [25]	4.696	23.254	46.775	8.807	27.253	49.420
Gupta et al. [18]	4.6963	23.2541	46.7745	8.8068	27.2529	49.4204
			h_0 = 0.15			
Present	4.8440	26.7148	59.0621	9.6286	33.3934	65.5507
Irie et al. [25]	4.844	26.715	59.062	9.629	33.393	65.551
Gupta et al. [18]	4.8440	26.7148	59.0621	9.6286	33.3934	65.5507
			h_0 = 0.05			
Present	4.9247	29.3233	71.7563	10.1447	38.8554	84.9950
Irie et al. [25]	4.925	29.323	71.756	10.145	38.855	84.995
Gupta et al. [18]	4.9247	29.3233	71.7563	10.1447	38.8554	84.9950

A comparative study of the frequency parameter Ω for homogeneous (α = 0, β = 0) isotropic (g = 0) Mindlin circular plates for N = 0, K_f = 0, γ = 0, with those of Irie et al. [25] obtained by Bessel functions and Gupta et al.[18] by Chebyshev collocation technique has been presented in Table 1. Similarly, for the critical buckling load parameter N_{cr} for homogeneous isotropic Mindlin plate, the computed results have been compared with those obtained by different methods: Wang et al. [43], Rao and Raju [34] and Hong et al. [20] and given in Table 2.

The numerical results have been presented in Tables 3-7 and Figs. 3-11. Tables 3 and 4 present the frequency parameter Ω for selected values of parameters : $g = 0, 5$; $N = -5, 0, 10, 20$; $\alpha = -0.5, 1$; $\beta = -0.5, 1$ obtained by first order shear deformation theory (FSDT, Ω_F) as well as classical plate theory (CPT, Ω_C) for fixed values of $K_f = 0.02$, $h_0 = 0.25$ and $\gamma = -0.5$ for both the boundary conditions. Here, it is worth to mention that in CPT, h_0 does not come into view clearly in the differential equation governing the motion apart from the final expression of Ω. Hence, the results for CPT have been calculated for a common value of h_0 and then converted to a desired value of h_0 by multiplying a factor $h_0/\sqrt{12}$. It is found from the results that the values of the frequency parameter Ω for a SS boundary condition are less than those for a corresponding C boundary condition. The values of the critical buckling loads for a C boundary condition are higher than that for the corresponding SS boundary condition. The values of the frequency parameter so obtained by FSDT are always lower than the corresponding frequencies obtained by CPT irrespective of the boundary conditions as well as other parameters.

Table 2
N_{cr} for homogeneous ($\alpha = 0, \beta = 0$) isotropic ($g = 0$) Mindlin circular plates taking $K_f = 0$, $\gamma = 0$.

h_0	SS-plate				C-plate			
	Present	Wang et al. [43]	Rao and Raju [34]	Hong et al. [20]	Present	Wang et al. [43]	Rao and Raju [34]	Hong et al. [20]
0.001	4.1978	4.1978	4.1978	4.1978	14.6819	14.6819	14.6826	14.6819
0.01	4.1973	4.1973	-	4.1973	14.6758	14.6759	-	14.6758
0.02	4.1958	4.1958	-	4.1958	14.6574	14.6574	-	14.6574
0.05	4.1852	4.1853	4.1852	4.1853	14.5296	14.5296	14.5299	14.5296
0.10	4.1480	4.1480	4.1481	4.1480	14.0909	14.0909	14.0910	14.0909
0.15	4.0875	4.0875	4.0874	4.0875	13.4157	13.4157	13.4159	13.4158
0.20	4.0056	4.0056	4.0054	4.0056	12.5724	12.5725	12.5725	12.5724

Table 3
Values of frequency parameter Ω for SS-plate for $h_0 = 0.25$, $\gamma = -0.5$, $K_f = 0.02$.

g	α		- 0.5				1			
	β		- 0.5		1		- 0.5		1	
	N	Modes	Ω_C	Ω_F	Ω_C	Ω_F	Ω_C	Ω_F	Ω_C	Ω_F
0	- 5	I	0.2063	0.1651	0.1469	0.1160	0.5339	0.4927	0.3841	0.3508
		II	2.5267	1.7094	1.7742	1.1794	3.7952	2.6348	2.7451	1.9027
		III	6.5107	3.4252	4.5220	2.3226	9.4737	5.0977	6.7576	3.6336
	0	I	0.4436	0.4184	0.3157	0.2936	0.6631	0.6254	0.4767	0.4444
		II	2.6842	1.9173	1.8840	1.3211	3.9061	2.7831	2.8242	2.0041
		III	6.6643	3.6864	4.6296	2.5003	9.5857	5.2936	6.8388	3.7655
	10	I	0.7108	0.6858	0.5054	0.4803	0.8655	0.8291	0.6213	0.5874
		II	2.9743	2.2758	2.0854	1.5643	4.1186	3.0551	2.9752	2.1889
		III	6.9613	4.1577	4.8372	2.8197	9.8056	5.6598	6.9980	4.0110
	20	I	0.9020	0.8749	0.6408	0.6119	1.0287	0.9916	0.7376	0.7010
		II	3.2384	2.5837	2.2680	1.7722	4.3201	3.3018	3.1178	2.3555
		III	7.2461	4.5777	5.0357	3.0958	10.0205	5.9981	7.1530	4.2370
5	- 5	I	*	*	*	*	0.1947	0.1373	0.1403	0.0983
		II	1.6967	0.8956	1.1920	0.6187	2.6944	1.6497	1.9498	1.2014
		III	4.6632	1.9591	3.2376	1.3247	6.9059	3.2084	4.9244	2.3013
	0	I	0.3290	0.3143	0.2342	0.2206	0.4917	0.4640	0.3535	0.3300
		II	1.9900	1.3471	1.3967	0.9275	2.8959	1.9529	2.0938	1.4086
		III	4.9408	2.5205	3.4323	1.7069	7.1066	3.6182	5.0701	2.5754
	10	I	0.7173	0.6989	0.5094	0.4887	0.8056	0.7784	0.5774	0.5501
		II	2.4742	1.9556	1.7321	1.3400	3.2601	2.4343	2.3519	1.7331
		III	5.4536	3.3660	3.7901	2.1060	7.4911	4.2952	5.3479	3.0249
	20	I	0.9595	0.9365	0.6808	0.6536	1.0276	0.9976	0.7350	0.7025
		II	2.8779	2.4102	2.0097	1.6449	3.5859	2.8260	2.5807	1.9949
		III	5.9219	3.8700	4.1150	2.1156	7.8557	4.8602	5.6096	3.3944

* denotes that the Ω does not exist due to buckling.

Table 4
Ω for C-plate for $h_0 = 0.25$, $\gamma = -0.5$, $K_f = 0.02$.

g	α		- 0.5				1			
	β		- 0.5		1		- 0.5		1	
	N	Modes	Ω_C	Ω_F	Ω_C	Ω_F	Ω_C	Ω_F	Ω_C	Ω_F
0	- 5	I	0.8476	0.6437	0.6457	0.4797	1.4875	1.1667	1.1577	0.8947
		II	3.4814	1.9718	2.4662	1.3279	5.2867	3.1509	3.8493	2.2366
		III	7.8890	3.5425	5.5042	2.3658	11.5744	5.4308	8.2858	3.8068
	0	I	0.9544	0.7638	0.7248	0.5649	1.5589	1.2483	1.2111	0.9527
		II	3.6115	2.1583	2.5610	1.4572	5.3829	3.2887	3.9207	2.3306
		III	8.0263	3.7949	5.6031	2.5382	11.6775	5.6201	8.3623	3.9334
	10	I	1.1353	0.9540	0.8579	0.6985	1.6908	1.3924	1.3092	1.0542
		II	3.8580	2.4895	2.7397	1.6856	5.5697	3.5436	4.0591	2.5038
		III	8.2940	4.2526	5.7956	2.8493	11.8809	5.9748	8.5131	4.1703
	20	I	1.2886	1.1083	0.9696	0.8062	1.8111	1.5182	1.3981	1.1422
		II	4.0892	2.7808	2.9063	1.8856	5.7498	3.7769	4.1919	2.6618
		III	8.5531	4.6619	5.9815	3.1252	12.0807	6.3033	8.6607	4.3893
5	- 5	I	0.4949	0.2629	0.3788	0.1993	1.0234	0.7214	0.7987	0.5582
		II	2.4399	1.0828	1.7251	0.7202	3.8175	1.9764	2.7777	1.4058
		III	5.7036	2.0273	3.9758	1.3493	8.4730	3.4002	6.0626	2.3963
	0	I	0.7076	0.5446	0.5374	0.4013	1.1558	0.8860	0.8979	0.6748
		II	2.6775	1.4811	1.8986	0.9968	3.9908	2.2582	2.9068	1.5969
		III	5.9505	2.5711	4.1540	1.7222	8.6575	3.7969	6.1997	2.6609
	10	I	0.9964	0.8455	0.7487	0.6112	1.3761	1.1251	1.0611	0.8412
		II	3.0968	2.0584	2.2015	1.3935	4.3144	2.7145	3.1458	1.9042
		III	6.4156	3.3990	4.4879	2.2835	9.0143	4.4564	6.4636	3.0996
	20	I	1.2121	1.0589	0.9043	0.7599	1.5597	1.3100	1.1956	0.9689
		II	3.4635	2.5028	2.4631	1.6963	4.6129	3.0908	3.3639	2.1569
		III	6.8485	4.0396	4.7965	2.7003	9.3565	5.0098	6.7152	3.4672

Figs. 3(a, b, c) depict the performance of gradient index g on Ω obtained by FSDT as well as CPT for two values of $\gamma = -0.5, 0.5$ for fixed values of $h_0 = 0.25$, $\alpha = 1$, $\beta = -0.5$, $K_f = 0.04$ and $N = 20$ for both the plates. It has been noticed that the value of Ω decreases with the increasing value of g for both the values of taper parameter γ except for $\gamma = 0.5$ in the two cases: (i) for both the plates vibrating in the first mode, (ii) for C-plate only in case of second mode. In the first case, the frequency parameter increases continuously with the increasing values of g while in the second case, there is a point of minima in the neighbourhood of $g = 1$. The rate of decrement in the values of frequency parameter with increasing values of g is much higher for the smaller values of i.e. $g \leq 2$ in comparison to the higher values $g > 2$. Further, this rate increases with the increasing number of modes. The effect of rotatory inertia and transverse shear decreases as the metal constituent in the plate material increases and plate becomes thinner and thinner towards the boundary i.e. as the values of g and γ increases. This effect further increases as the number of modes increases.

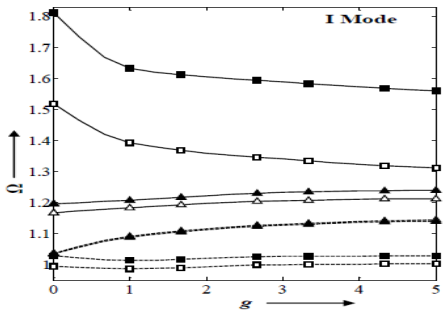

(a)

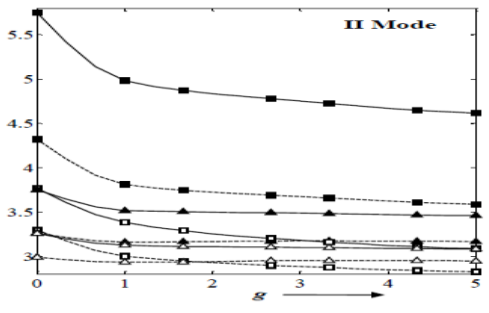

(b)

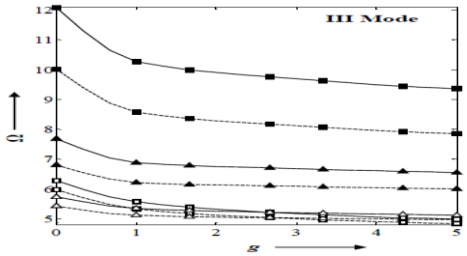

(c)

Fig.3
Frequency parameter Ω for $h_0 = 0.25$, $\alpha = 1$, $\beta = -0.5$, $K_f = 0.04$, $N = 20$, _ _ _ _ _, SS-plate; _____, C-plate; FSDT- □, γ = - 0.5 ; △, γ = 0.5; CPT- ■, γ = - 0.5; ▲, γ = 0.5.

To observe the effect of loading parameter N on the frequency parameter Ω, the graphs have been plotted for fixed values of $h_0 = 0.25$, $\alpha = 1$, $\beta = -0.5$, $K_f = 0.04$ for two values of $g = 0$, 5 and γ = - 0.5, 0.5 and given in Figs. 4(a, b, c) for all the modes for both the boundary conditions. It has been observed that the value of the frequency parameter increases with the increasing value of loading parameter whatsoever be the values of other parameters fixed for both the plates. The rate of increase in the values of Ω with N decreases as the plate becomes thicker and thicker towards the boundary i.e. γ changes from 0.5 to - 0.5 for both the boundary conditions. This effect is higher for FGM plate i.e. $g = 5$ as compared to isotropic plate i.e. $g = 0$ and is more prominent for the C-plates as compared to the SS ones.

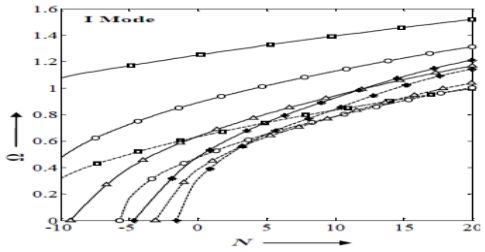

(a)

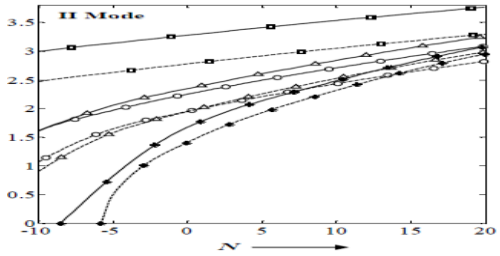

(b)

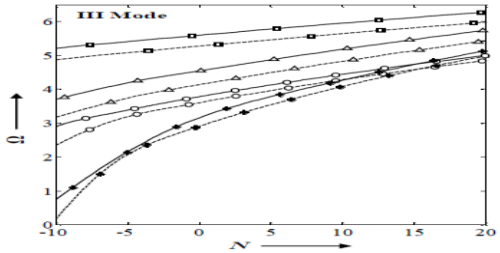

(c)

Fig.4
Ω for $h_0 = 0.25$, $\beta = -0.5$, $\alpha = 1$, $K_f = 0.04$;_ _ _ _ _, SS-plate; _____, C-plate; □ , $g = 0$, γ = - 0.5; Δ , $g = 0$, γ = 0.5; ○ , $g = 5$, γ = - 0.5; ✱ , $g = 5$, γ = 0.5.

To observe the effect of foundation parameter on the frequencies, the graphs Ω verses K_f for two different values of N = - 5, 10 and γ = - 0.5, 0.5 for $h_0 = 0.25$, $\alpha = 1$, $\beta = -0.5$ and $g = 5$ for all the three modes have been presented in Figs. 5(a, b, c). It can be seen that Ω increases with the increasing values of K_f for both the plates whatsoever be the values of the other parameters. The effect is higher in case of SS-plate in comparison to the C-plate for the same set of other parameters and increases as the number of modes increase.

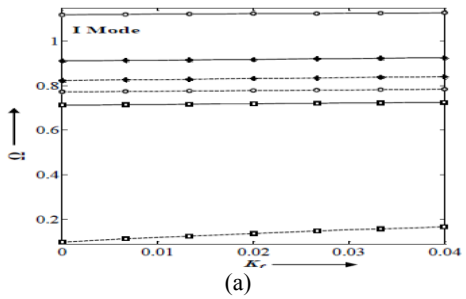

(a)

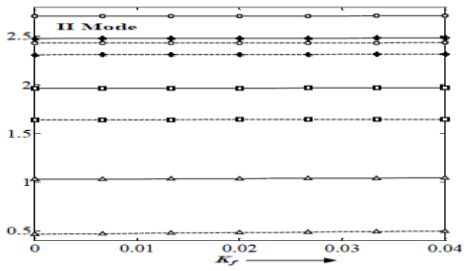

(b)

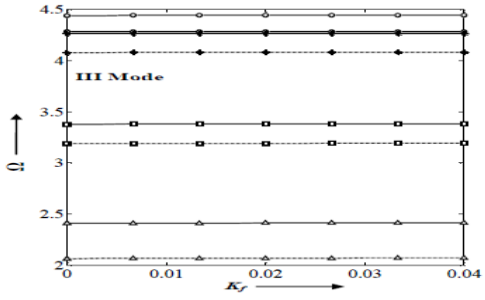

(c)

Fig.5
Ω for $h_0 = 0.25$, $\alpha = 1$, $g = 5$, $\beta = -0.5$; _ _ _ _ _, SS-plate; _____, C-plate; ○ , N= 10, γ = -0.5; Δ , N= -5, γ = 0.5; □ , N= -5, γ = - 0.5; ✱ , N= 10, γ = 0.5.

The behaviour of taper parameter γ on the frequency parameter Ω has been shown in Figs. 6(a, b, c) for fixed values of $\alpha = 1$; $\beta = -0.5$; $K_f = 0.04$; $N = 20$ and $g = 5$ for two values of $h_0 = 0.15$, 0.25 for all the three modes for both the plates. For the first mode of vibration, the values of frequency parameter Ω_F increase monotonically with the increasing values of γ for SS-plates while for C-plates, it is just the reverse. In case of second mode, the graphs show that the behaviour of Ω_F with taper parameter γ has a point of minima for $h_0 > 0.15$ in the vicinity of γ = 0.1 for both the plates and γ = 0.3 for $h_0 < 0.15$ only for SS-plate. For the third mode of vibration, the value of Ω_F decreases with the increasing values of γ for $h_0 \leq 0.15$ whereas monotonically increases for $h_0 > 0.15$. It is worth to mention that the difference between Ω_C and Ω_F i.e. $(\Omega_C - \Omega_F)$ decreases as the plates become thinner and thinner towards the boundary for all the modes.

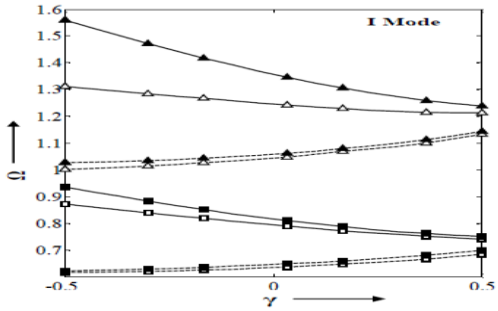

(a)

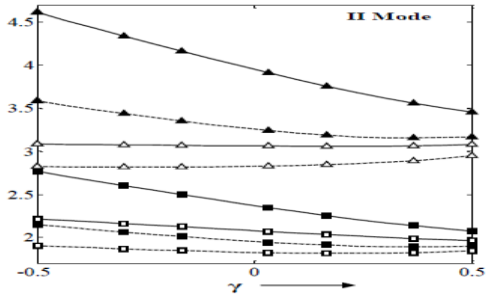

(b)

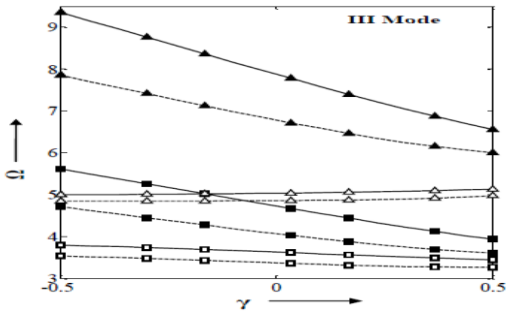

(c)

Fig.6
Ω for $\alpha = 1$, $\beta = -0.5$, $K_f = 0.04$, $N = 20$, $g = 5$; _ _ _ _ _, SS-plate; _____, C-plate; FSDT- □, $h_0 = 0.15$; △, $h_0 = 0.25$; CPT- ■, $h_0 = 0.15$; ▲, $h_0 = 0.25$.

The plots of frequency parameter Ω with varying values of heterogeneity parameter α for two values of γ = - 0.5, 0.5 and $\beta = -0.5$, 1 for fixed values of $h_0 = 0.25$; $g = 5$; $K_f = 0.04$ and $N = 20$ have been drawn in Figs. 7(a, b, c). It can be clearly seen that Ω increases as the stiffness of the plate in R-direction increases i.e. as α varies from - 0.5 to 1 for all the modes for both the boundary conditions. This effect is more pronounced for C-plate as compared to the corresponding SS-plate. The rate of increase in the values of frequency parameter Ω with the heterogeneity parameter α increases as the plate becomes thicker and thicker towards the boundary i.e. γ changes from 0.5 to - 0.5 and increases with the increase in the number of modes.

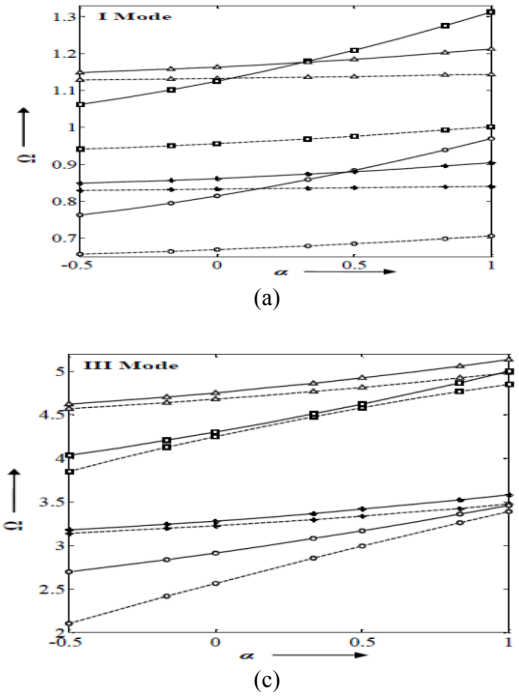

Fig.7
Ω for h_0 = 0.25, g = 5, K_f = 0.04, N = 20; _ _ _ _ _, SS-plate; _____, C-plate; □ , β= - 0.5, γ = - 0.5; Δ , β= - 0.5, γ = 0.5; ○ , β= 1, γ = - 0.5; ✱, β=1, γ = 0.5.

Figs. 8(a, b, c) demonstrate the effect of density parameter β on frequency parameter Ωtaking two values of γ = - 0.5, 0.5 and α = - 0.5, 1 for fixed values of h_0 = 0.25; g = 5; K_f = 0.04 and N = 20 for both the plates and for all the three modes of vibration. From the graphs, it has been noted that the frequency parameter decreases continuously with the increasing values of density parameter β. The rate of decrease in the values of Ω with β increases with the increase in the number of modes.

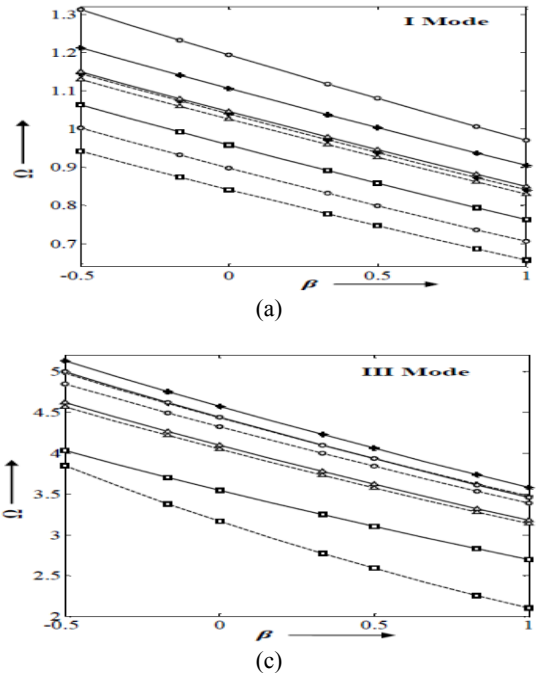

Fig.8
Ω for h_0 = 0.25, g = 5, K_f = 0.04, N = 20; _ _ _ _ _, SS-plate; _____, C-plate; □ , α= -0.5, γ = - 0.5; Δ , α= - 0.5, γ = 0.5; ○ , α = 1, γ = - 0.5; ✱, α = 1, γ = 0.5.

To study the effect of thickness variation h_0 on the frequency parameter Ω, the results obtained by FSDT and CPT have been plotted for two values of γ = - 0.5, 0.5 and K_f = 0, 0.02 for fixed values of α = 1; β = - 0.5; N = 20 and g = 5 for all the three modes in Figs. 9(a, b). It is noticed that the frequency parameter Ω increases with the

increase in the values of thickness parameter h_0 for both the plates which may be accredited to the increased inertia of the plate. This effect is more obvious for a C-plate in comparison to SS-plate due to edge fixidity condition. Beyond this, it can be seen that the effect of rotatory inertia and transverse shear increases with the increase in the number of modes as well as with the values of h_0. And, it decreases as the value of taper parameter γ increases from - 0.5 to 0.5 for both the plates and all the modes. However, the increase in the value of K_f, increases this effect for both the plates.

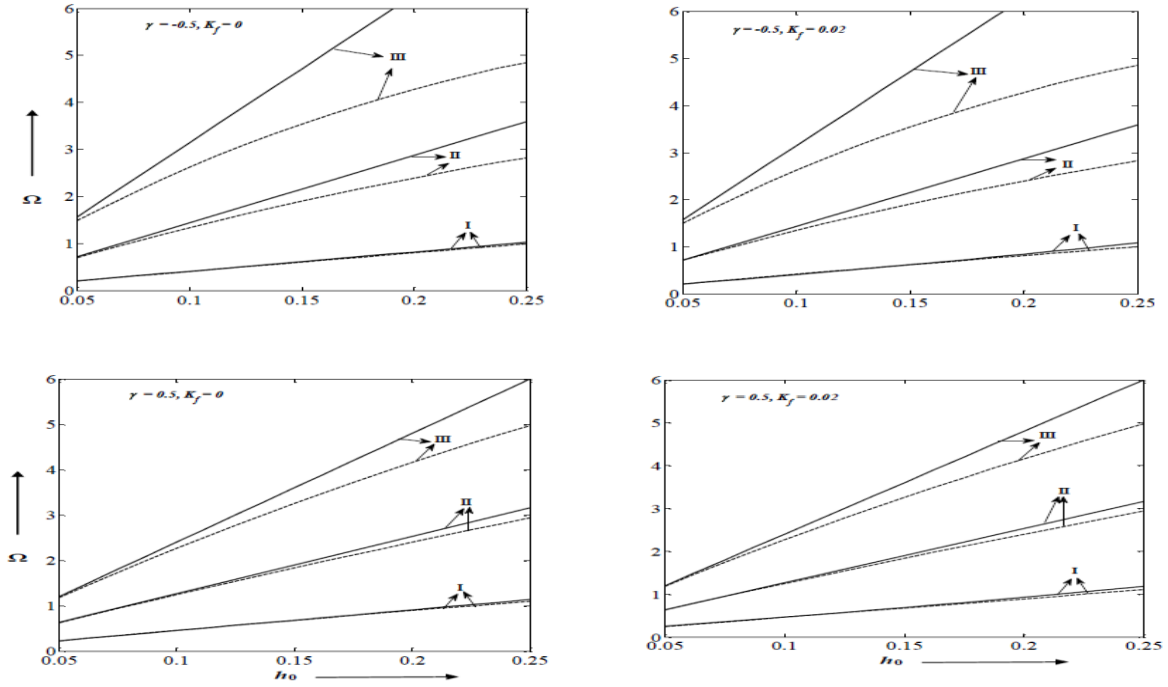

Fig.9
(a) Ω for SS-plate; _ _ _ _, FSDT; _____, CPT.

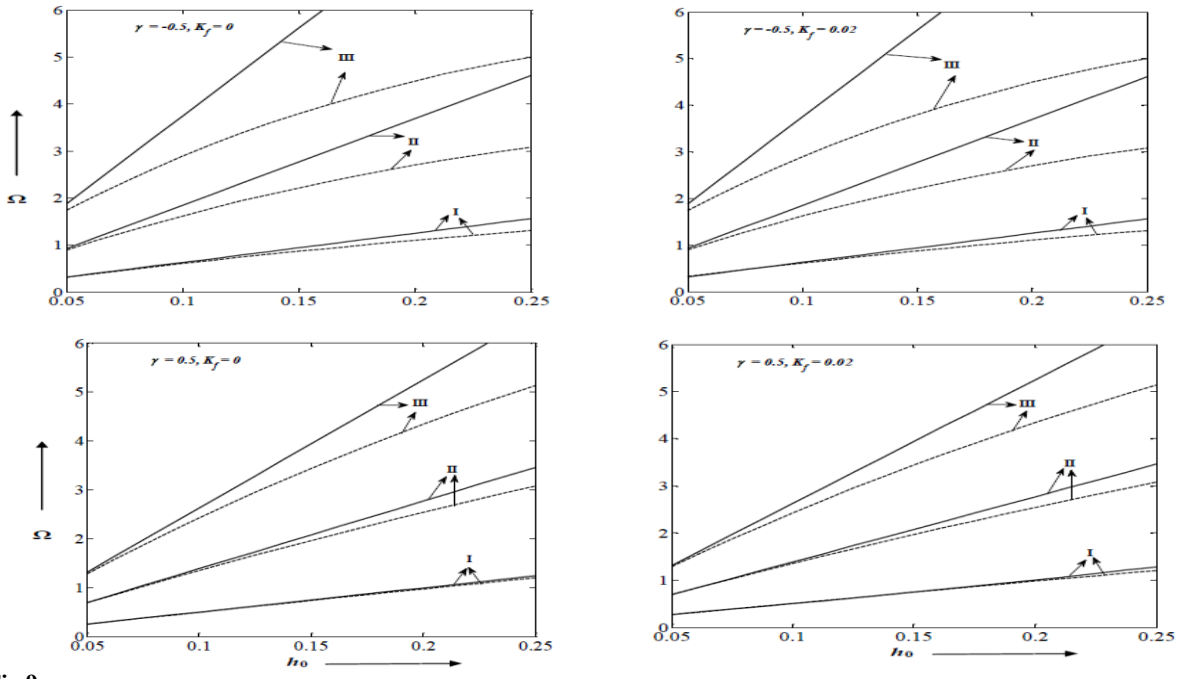

Fig.9
(b) Ω for C-plate; _ _ _ _, FSDT; _____, CPT.

The percentage variation in the values of frequency parameters obtained by CPT (Ω_C) and FSDT (Ω_F) i.e. $(\Omega_C - \Omega_F)\times 100/\Omega_F$, for various combinations of the values of K_f = 0, 0.02 and g = 0, 5 with varying values of h_0 = 0.05, 0.10, 0.15, 0.25 for fixed values of N = 20, α = 1, β = - 0.5, γ = -0.5 have been computed and presented in Table 5. The results reveal that CPT fails to predict satisfactory results even for the second mode for C-plate provided $h_0 > 0.10$ as the error is more than 10 %. In case of SS boundary condition, the percentage error is less as compared to that for C boundary condition for the same set of the values of other parameters. Thus, one can decide the applicability range of CPT by choosing appropriate values of other parameters including h_0.

Table 5
The percentage variation of Ω_C and Ω_F i.e. $(\Omega_C - \Omega_F)\times 100/\Omega_F$.

Boundary Conditions	K_f	g	Modes	h_0			
				0.05	0.10	0.15	0.25
SS-plate	0	0	I	0.15	0.68	1.55	4.08
			II	1.87	6.86	14.01	31.19
			III	4.78	16.92	32.85	67.58
		5	I	0.47	0.61	1.35	3.44
			II	1.90	6.75	13.29	27.19
			III	5.24	17.91	33.18	62.08
	0.02	0	I	0.07	1.39	0.60	3.71
			II	1.38	6.71	13.94	31.15
			III	4.68	16.88	32.84	67.57
		5	I	0.09	0.10	0.11	2.99
			II	0.94	6.49	13.15	27.12
			III	5.03	17.83	33.14	61.99
C-plate	0	0	I	0.97	3.78	8.11	19.65
			II	3.27	12.05	24.30	52.68
			III	6.83	23.87	45.75	92.32
		5	I	1.07	4.14	8.61	19.54
			II	3.64	13.00	25.13	49.64
			III	7.85	26.29	47.92	87.29
	0.02	0	I	1.68	3.04	7.73	19.47
			II	2.97	11.96	24.24	52.65
			III	6.76	23.84	45.73	92.30
		5	I	1.86	2.82	7.95	19.22
			II	3.04	12.81	25.01	49.57
			III	7.69	26.23	47.87	87.25

The values of the N_{cr} in compression have been calculated by putting the frequency to zero, for g = 0, 1, 3, 5; K_f = 0.02, 0.04; α = - 0.5, 0, 1 and γ = - 0.5, 0.5 for h_0 = 0.25 and given in Tables 6 and 7. Here, it is important to mention that the value of N_{cr} does not depend upon the density parameter β. For selected values of K_f = 0.02, 0.04; h_0 = 0.05, 0.15; γ = - 0.5, 0.5; α = 1; β = - 0.5; g = 5, the graphs for the critical buckling load parameter N_{cr} for both the plates vibrating in the first mode of vibration have been plotted in Figs. 10 (a, b). From the results, it has been noticed that the value of the N_{cr} for a SS-plate are lower than that for the corresponding C-plate. The value of N_{cr} increases with the increasing values of heterogeneity parameter α and foundation parameter K_f for both the plates whereas the value of N_{cr} decreases as the thickness parameter h_0 as well as gradient index g increases whatsoever be the value of the other plate parameters.

Table 6
Values of N_{cr} for SS-plate for h_0 = 0.25.

		γ = - 0.5					
K_f		0.02			0.04		
g	α	- 0.5	0	1	- 0.5	0	1
0	I	5.9218	7.6983	13.1551	6.1540	7.9303	13.3846
	II	24.2692	30.8051	44.7362	24.3131	30.8470	44.7695
	III	36.2803	45.1495	56.1037	36.2965	45.1637	56.1061
1	I	3.6010	4.6529	7.8828	3.8332	4.8849	8.1122
	II	14.3878	18.2570	26.5021	14.4318	18.2989	26.5355
	III	21.4883	26.7384	33.2204	21.5049	26.7564	33.2229

	I	2.8457	3.6680	6.1867	3.0778	3.9000	6.4157
3	II	10.4443	13.2329	18.8782	10.4883	13.2745	18.9091
	III	14.9512	18.5214	21.9299	14.9754	18.5412	21.9305
	I	2.5314	3.2571	5.4775	2.7635	3.4891	5.7063
5	II	8.9437	11.3232	16.0279	8.9877	11.3647	16.0576
	III	12.6165	15.5722	18.1133	12.5930	15.6224	18.1136
				$\gamma = 0.5$			
	K_f		0.02			0.04	
g	α	- 0.5	0	1	- 0.5	0	1
	I	1.3874	1.7742	2.8955	1.6045	1.9963	3.1242
0	II	5.8426	8.0386	14.5857	5.8916	8.0866	14.6322
	III	10.8874	15.3138	27.8768	10.9050	15.3321	27.8954
	I	0.9101	1.1412	1.8077	1.1259	1.3627	2.0363
1	II	3.4794	4.7792	8.6552	3.5295	4.8278	8.7018
	III	6.4537	9.0748	16.5136	6.4714	9.0931	16.5322
	I	0.7602	0.9439	1.4719	0.9745	1.1647	1.7005
3	II	2.6409	3.6352	6.5898	2.6916	3.6842	6.6365
	III	4.6693	6.6134	12.0764	4.6864	6.6315	12.0950
	I	0.6969	0.8604	1.3295	0.9102	1.0808	1.5579
5	II	2.3036	3.1733	5.7532	2.3550	3.2225	5.8000
	III	3.9908	5.6702	10.3692	4.0077	5.6882	10.3879

Table 7
Values of N_{cr} for C-plate for $h_0 = 0.25$

				$\gamma = - 0.5$			
	K_f		0.02			0.04	
g	α	- 0.5	0	1	- 0.5	0	1
	I	16.3323	21.3181	34.2207	16.5042	21.4734	34.3351
0	II	31.4523	39.5330	53.8878	31.4831	39.5862	53.9137
	III	35.2472	49.5859	56.8240	40.0156	49.5115	56.9822
	I	9.7406	12.6859	20.3090	9.9117	12.8405	20.4230
1	II	18.6303	23.4294	31.9186	18.6901	23.4827	31.9451
	III	23.7854	29.2449	33.6460	23.8870	29.3358	33.7410
	I	7.3160	9.4923	14.9837	7.4864	9.6449	15.0918
3	II	13.1952	16.5367	21.7532	13.2554	16.5886	21.7650
	III	16.0609	24.4987	22.1403	15.9451	20.0321	22.2533
	I	6.3569	8.2318	12.9089	6.5267	8.3834	13.0142
5	II	11.1935	14.0059	18.0968	11.2539	14.0570	18.1068
	III	13.6911	16.7321	18.3303	13.8654	16.7244	18.4440
				$\gamma = 0.5$			
	K_f		0.02			0.04	
g	α	- 0.5	0	1	- 0.5	0	1
	I	3.2981	4.4243	7.9199	3.5093	4.6330	8.1183
0	II	8.4607	11.7409	21.3151	8.5016	11.7853	21.3644
	III	12.9317	18.3947	33.5204	12.9550	18.4181	33.5435
	I	2.0390	2.7048	4.7704	2.2494	2.9128	4.9684
1	II	5.0263	6.9699	12.6409	5.0673	7.0144	12.6904
	III	7.6664	10.9011	19.8570	7.6901	10.9247	19.8801
	I	1.6254	2.1427	3.7442	1.8348	2.3502	3.9417
3	II	3.7305	5.1939	9.4322	3.7713	5.2384	9.4818
	III	5.4411	7.8109	14.2850	5.4651	7.8348	14.3080
	I	1.4537	1.9092	3.3173	1.6626	2.1162	3.5144
5	II	3.2229	4.4948	8.1660	3.2637	4.5393	8.2157
	III	4.6151	6.6525	12.1869	4.6393	6.6765	12.2099

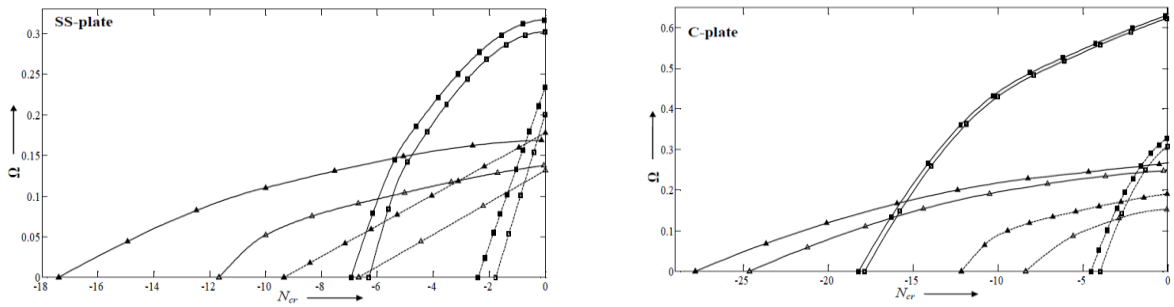

(a) (b)

Fig.10

N_{cr} for $\alpha = 1$, $\beta = -0.5$, $g = 5$; _____, $\gamma = -0.5$; _ _ _ _ _, $\gamma = 0.5$; Δ, $h_0 = 0.05$, $K_f = 0.02$; □, $h_0 = 0.15$, $K_f = 0.02$; ▲, $h_0 = 0.05$, $K_f = 0.04$; ■, $h_0 = 0.15$, $K_f = 0.04$.

3 dimensional mode shapes for first three frequency parameters for a particular plate $N = 20$, $g = 5$, $h_0 = 0.25$, $\alpha = 1$, $\beta = -0.5$, $\gamma = 0.5$, $K_f = 0.02$ are shown in Figs. 11(a, b) for both the boundary conditions.

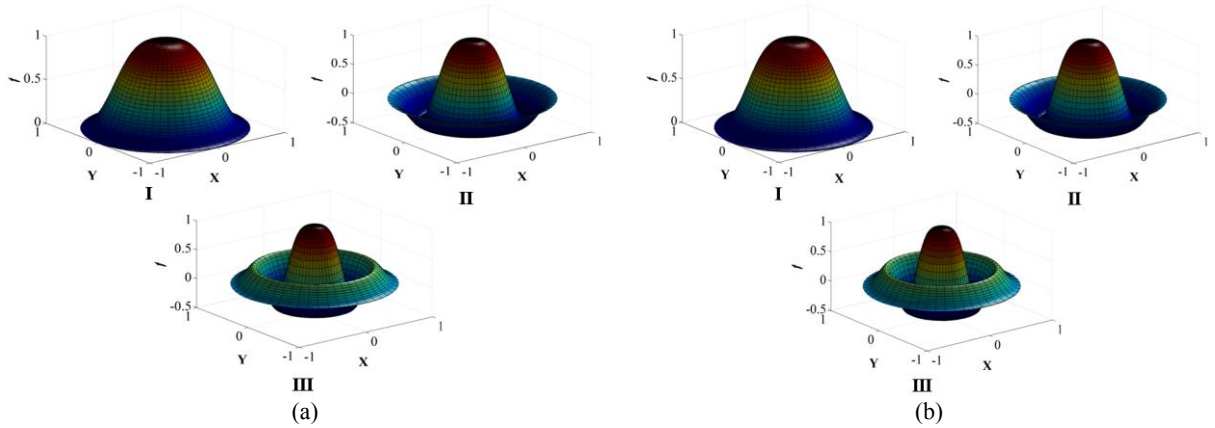

(a) (b)

Fig.11

3D mode shapes for $N = 20$, $g = 5$, $h_0 = 0.25$, $\alpha = 1$, $\beta = -0.5$, $\gamma = 0.5$, $K_f = 0.02$; (a) SS-plate (b) C-plate.

In order to study the effect of rotatory inertia and transverse shear individually, the results were computed by neglecting rotatory inertia term i.e. by putting $k_1 = 0$ in Eq. (1a). It was noticed that the computed value of Ω differ negligibly from the corresponding value of Ω_F, leading to the conclusion that transverse shear deformation amounts almost the entire discrepancy. As Ω_F is always less than the corresponding values of Ω_C for both the plates whatsoever be the values of other parameters, therefore, the effect of rotatory inertia and transverse shear must be taken into account in studying the dynamic response of moderately thick FGM plates i.e. $h_0 > 0.1$.

5 CONCLUSIONS

The effect of Winkler foundation and uniform in-plane peripheral loading has been studied on the buckling and vibration characteristics of bi-directional moderately thick FGM circular plates of linearly varying thickness. Observing the results, these subsequent conclusions have been made –

1. The increase in the values of heterogeneity parameter gives rise a stiffer and stiffer plate in the *R*-direction and ultimately the frequency parameter increases.
2. As the plate becomes denser in the *R*-direction by increasing the values of density parameter, the value of the frequency parameter decreases.
3. The frequency parameter increases continuously for both the plates as the stiffness of the Winkler foundation increases keeping the other parameters fixed.

4. With the increase in the values of plate thickness, the value of the frequency parameter increases continuously due to the increase inertia of the plate.
5. The effect of rotatory inertia and transverse shear is more evident for an isotropic plate in comparison to the corresponding FGM plate for both the boundary conditions. Also, it is more prominent when the plate is thick at the boundary as compared to the centre.
6. The percentage decrease in the values of Ω_F with respect to the corresponding Ω_C i.e. $\left(\Omega_C - \Omega_F\right)\times 100/\Omega_F$ increases with the increasing values of thickness parameter h_0 for both the boundary conditions and all the modes.

The overall analysis shows that the CPT overpredicts the frequency as compared to FSDT for FGM plates. A similar interference was obtained by Deresiewicz and Mindlin [9] for isotropic circular disks, Lal and Gupta [26] for polar orthotropic annular plates of parabolically varying thickness and Gupta et al. [18] for non-homogeneous circular plates of quadratically varying thickness. Thus, the effect of transverse shear and rotatory inertia should be taken into consideration in analysing the dynamic buckling of two-directional FGM moderately thick circular plates of variable thickness resting on Winkler foundation with a fair amount of accuracy.

REFERENCES

[1] Amini M.H., Soleimani M., Rastgoo A., 2009, Three-dimensional free vibration analysis of functionally graded material plates resting on an elastic foundation, *Smart Materials and Structures* **18**(8): 085015.

[2] Ansari R., Gholami R., Shojaei M.F., Mohammadi V., Darabi M.A., 2013, Thermal buckling analysis of a Mindlin rectangular FGM microplate based on the strain gradient theory, *Journal of Thermal Stresses* **36**(5): 446-465.

[3] Baferani A.H., Saidi A.R., Jomehzadeh E., 2011, An exact solution for free vibration of thin functionally graded rectangular plates, *Proceedings of the Institution of Mechanical Engineers Part C, Journal of Mechanical Engineering Science* **225**(3): 526-536.

[4] Batra R.C., Aimmanee S., 2005, Vibrations of thick isotropic plates with higher order shear and normal deformable plate theories, *Computers and Structures* **83**: 934-955.

[5] Bisadi H., Es' haghi M., Rokni H., Ilkhani M., 2012, Benchmark solution for transverse vibration of annular Reddy plates, *International Journal of Mechanical Sciences* **56**(1): 35-49.

[6] Bowles J.E., 1982, *Foundation Analysis and Design,* McGraw-Hill, Inc.

[7] Chen S.S., Xu C.J., Tong G.S., Wei X., 2015, Free vibration of moderately thick functionally graded plates by a meshless local natural neighbor interpolation method, *Engineering Analysis with Boundary Elements* **61**: 114-126.

[8] Civalek Ö., 2008, Free vibration analysis of symmetrically laminated composite plates with first-order shear deformation theory (FSDT) by discrete singular convolution method, *Finite Elements in Analysis and Design* **44**(12): 725-731.

[9] Deresiewicz H., Mindlin R.D., 1955, Axially symmetric flexural vibrations of a circular disk, *Journal of Applied Mechanics* **22**: 86-88.

[10] Efraim E., 2011, Accurate formula for determination of natural frequencies of FGM plates basing on frequencies of isotropic plates, *Procedia Engineering* **10**: 242-247.

[11] Efraim E., Eisenberger M., 2007, Exact vibration analysis of variable thickness thick annular isotropic and FGM plates, *Journal of Sound and Vibration* **299**(4): 720-738.

[12] Eftekhari S.A., Jafari A.A., 2013, Modified mixed Ritz-DQ formulation for free vibration of thick rectangular and skew plates with general boundary conditions, *Applied Mathematical Modelling* **37**(12): 7398-7426.

[13] Fallah A., Aghdam M.M., Kargarnovin M.H., 2013, Free vibration analysis of moderately thick functionally graded plates on elastic foundation using the extended Kantorovich method, *Archive of Applied Mechanics* **83**(2): 177-191.

[14] Ferreira A.J.M., Roque C.M.C., Jorge R.M.N., 2005, Free vibration analysis of symmetric laminated composite plates by FSDT and radial basis functions, *Computer Methods in Applied Mechanics and Engineering* **194**(39): 4265-4278.

[15] Gorman D.G., 1983, Vibration of thermally stressed polar orthotropic annular plates, *Earthquake Engineering and Structural Dynamics* **11**(6): 843-855.

[16] Gupta U.S., Lal R., 1979, Axisymmetric vibrations of linearly tapered annular plates under an in-plane force, *Journal of Sound and Vibration* **64**(2): 269-276.

[17] Gupta U.S., Ansari A.H., Sharma S., 2006, Buckling and vibration of polar orthotropic circular plate resting on Winkler foundation, *Journal of Sound and Vibration* **297**(3): 457-476.

[18] Gupta U.S., Lal R., Sharma S., 2007, Vibration of non-homogeneous circular Mindlin plates with variable thickness, *Journal of Sound and Vibration* **302**(1): 1-17.

[19] Han J.B., Liew K.M., 1999, Axisymmetric free vibration of thick annular plates, *International Journal of Mechanical Sciences* **41**(9): 1089-1109.

[20] Hong G.M., Wang C.M., Tan M.T., 1993, Analytical buckling solutions for circular Mindlin plates: inclusion of inplane prebuckling deformation, *Archive of Applied Mechanics* **63**(8): 534-542.

[21] Hosseini-Hashemi S., Derakhshani M., Fadaee M., 2013, An accurate mathematical study on the free vibration of stepped thickness circular/annular Mindlin functionally graded plates, *Applied Mathematical Modelling* **37**(6): 4147-4164.
[22] Hosseini-Hashemi S., Fadaee M., Es' Haghi M., 2010, A novel approach for in-plane/out-of-plane frequency analysis of functionally graded circular/annular plates, *International Journal of Mechanical Sciences* **52**(8): 1025-1035.
[23] Hosseini-Hashemi S., Taher H.R.D., Akhavan H., 2010, Vibration analysis of radially FGM sectorial plates of variable thickness on elastic foundations, *Composite Structures* **92**(7): 1734-1743.
[24] Irie T., Yamada G., Aomura S., 1979, Free vibration of a Mindlin annular plate of varying thickness, *Journal of Sound and Vibration* **66**(2): 187-197.
[25] Irie T., Yamada G., Aomura S., 1980, Natural frequencies of Mindlin circular plates, *Journal of Applied Mechanics* **47**(3): 652-655.
[26] Lal R., Gupta U.S., 1982, Influence of transverse shear and rotatory inertia on axisymmetric vibrations of polar orthotropic annular plates of parabolically varying thickness, *Indian Journal of Pure and Applied Mathematics* **13**(02): 205-220.
[27] Leissa A.W., 1982, *Advances and Trends in Plate Buckling Research* , Ohio State University Research Foundation Columbus.
[28] Li S.Q., Yuan H., 2011, Quasi-Green's function method for free vibration of clamped thin plates on Winkler foundation, *Applied Mathematics and Mechanics* **32**: 265-276.
[29] Liew K.M., Hung K.C., Lim M.K., 1995, Vibration of Mindlin plates using boundary characteristic orthogonal polynomials, *Journal of Sound and Vibration* **182**(1): 77-90.
[30] Mindlin R.D., 1951, Influence of rotatory inertia and shear on flexural motions of isotropic, elastic plates, *Journal of Applied Mechanics* **18**: 31-38.
[31] Miyamoto Y., Kaysser W.A., Rabin B.H., Kawasaki A., Ford R.G., 2013, *Functionally Graded Materials: Design, Processing and Applications*, Springer Science & Business Media.
[32] Naderi A., Saidi A.R., 2011, An analytical solution for buckling of moderately thick functionally graded sector and annular sector plates, *Archive of Applied Mechanics* **81**(6): 809-828.
[33] Najafizadeh M.M., Heydari H.R., 2008, An exact solution for buckling of functionally graded circular plates based on higher order shear deformation plate theory under uniform radial compression, *International Journal of Mechanical Sciences* **50**: 603-612.
[34] Rao G.V., Raju K.K., 1986, A study of various effects on the stability of circular plates, *Computers and Structures* **24**(1): 39-45.
[35] Rao L.B., Rao C.K., 2014, Frequency analysis of annular plates with inner and outer edges elastically restrained and resting on Winkler foundation, *International Journal of Mechanical Sciences* **81**: 184-194.
[36] Saidi A.R., Baferani A.H., Jomehzadeh E., 2011, Benchmark solution for free vibration of functionally graded moderately thick annular sector plates, *Acta Mechanica* **219**(3-4): 309-335.
[37] Satouri S., Asanjarani A., Satouri A., 2015, Natural frequency analysis of 2D-FGM sectorial plate with variable thickness resting on elastic foundation using 2D-DQM, *International Journal of Applied Mechanics* **7**(02): 1550030.
[38] Striz A.G., Wang X., Bert C.W., 1995, Harmonic differential quadrature method and applications to analysis of structural components, *Acta Mechanica* **111**(1-2): 85-94.
[39] Su Z., Jin G., Wang X., 2015, Free vibration analysis of laminated composite and functionally graded sector plates with general boundary conditions, *Composite Structures* **132**: 720-736.
[40] Tajeddini V., Ohadi A., 2011, Three-dimensional vibration analysis of functionally graded thick, annular plates with variable thickness via polynomial-Ritz method, *Journal of Vibration and Control* **18**(11): 1698-1707.
[41] Thai H.T., Choi D.H., 2013, A simple first-order shear deformation theory for the bending and free vibration analysis of functionally graded plates, *Composite Structures* **101**: 332-340.
[42] Thai H.T., Kim S.E., 2015, A review of theories for the modeling and analysis of functionally graded plates and shells, *Composite Structures* **128**: 70-86.
[43] Wang C.M., Xiang Y., Kitipornchai S., Liew K.M., 1993, Axisymmetric buckling of circular Mindlin plates with ring supports, *Journal of Structural Engineering* **119**(3): 782-793.
[44] Wang Q., Shi D., Liang Q., Shi X., 2016, A unified solution for vibration analysis of functionally graded circular, annular and sector plates with general boundary conditions, *Composites Part B-Engineering* **88**: 264-294.
[45] Xiang Y., 2003, Vibration of rectangular Mindlin plates resting on non-homogenous elastic foundations, *International Journal of Mechanical Sciences* **45**(6): 1229-1244.
[46] Xiang Y., Wei G.W., 2004, Exact solutions for buckling and vibration of stepped rectangular Mindlin plates, *International Journal of Solids and Structures* **41**(1): 279-294.
[47] Xue K., Wang J.F., Li Q.H., Wang W.Y., Wang P., 2014, An exact series solution for the vibration of Mindlin rectangular plates with elastically restrained edges, *Key Engineering Materials* **572**: 489-493.
[48] Zamani M., Fallah A., Aghdam M.M., 2012, Free vibration analysis of moderately thick trapezoidal symmetrically laminated plates with various combinations of boundary conditions, *European Journal of Mechanics-A/Solids* **36**: 204-212.
[49] Zenkour A.M., 2005, A comprehensive analysis of functionally graded sandwich plates: Part 2—Buckling and free vibration, *International Journal of Solids and Structures* **42**(18): 5243-5258.

[50] Zhang L.W., Lei Z.X., Liew K.M., 2015, Buckling analysis of FG-CNT reinforced composite thick skew plates using an element-free approach, *Composites Part B: Engineering* **75**: 36-46.

[51] Zhang L.W., Lei Z.X., Liew K.M., 2015, Computation of vibration solution for functionally graded carbon nanotube-reinforced composite thick plates resting on elastic foundations using the element-free IMLS-Ritz method, *Applied Mathematics and Computation* **256**: 488-504.

[52] Zhao X., Lee Y.Y., Liew K.M., 2009, Mechanical and thermal buckling analysis of functionally graded plates, *Composite Structures* **90**: 161-171.